

T3a:

Star formation: maser variability *Chair: Philip Diamond*

Variability of Class II methanol masers in massive star forming regions

Sharmila Goedhart^{1,2}, Mike Gaylard², and Johan van der Walt³

¹SKA SA, Third Floor, The Park, Park Rd, Pinelands 7405, South Africa

²Hartebeesthoek Radio Astronomy Observatory, PO Box 443, Krugersdorp 1740, South Africa

³Centre for Space Research, North-West University, Private Bag X6001, Potchefstroom 2520, South Africa

Abstract. Class II methanol masers are known to be tracers of an early phase of massive star formation. The 6.7- and 12.2-GHz methanol maser transitions can show a significant amount of variability, including periodic variations. Studying maser variability can lead to important insights into conditions in the maser environment but first the maser time-series need to be characterised. The results of long-term monitoring of 8 regularly-varying sources will be presented and methods of period-search discussed.

Keywords. masers, radio lines: ISM, stars: formation

1. Introduction

Class II methanol masers are known to be tracers of the earliest stages of massive starformation (Breen *et al.*, 2010). In many cases the maser is the only readily detectable emission in the region of the massive young star. Masers are extremely sensitive to all changes in their environment. This would include local conditions in the masing gas volume as well as the incoming radiation field. Class II methanol masers are believed to be primarily pumped by infrared radiation (Cragg, Sobolev & Godfrey, 2005). Thus studying variability in methanol masers could lead to insights into changing conditions in massive star forming regions. Some methanol masers are known to be highly variable (e.g. Caswell, Vaile & Ellingsen 1995, MacLeod & Gaylard 1996).

The Hartebeesthoek Radio Astronomy Observatory has been monitoring a selection of methanol masers since 1992. The source G351.78-0.54 has now been monitored for 19 years. In 1999, Goedhart, Gaylard & van der Walt (2004) started an intensive program to monitor 54 methanol maser sources over four years. The sample showed a range of behaviour, including the very surprising result of periodicity in six of the sources. Monitoring continues on sources of interest. The time-series on G351.78-0.54 and the periodic sources will be discussed.

2. Observations

The observations were done using the 26-m telescope at the Hartebeesthoek Radio Astronomy Observatory. The observations from September 1992 to April 2003 were of left-circular polarisation using a 256-channel spectrometer. Observations resumed in September 2003 with the cryogenic receiver upgraded from single to dual polarisation, a 2x1024 channel spectrometer and a new telescope control system. The telescope surface was replaced by solid panels, with the final alignment taking place in September 2004. Amplitude calibrations were based on continuum monitoring of Virgo A, Hydra A and 3C123. Pointing corrections were calculated by observing at half a beamwidth

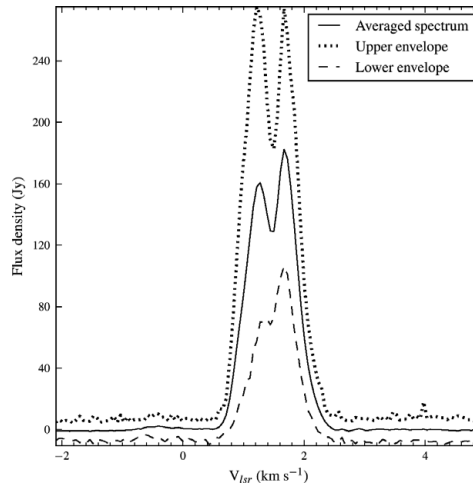


Figure 1. Range of variation of G351.78-0.54.

offset to the north, south, east and west of the source position. The calibrations were checked against the relatively quiescent source G351.42+0.64. The sources were generally observed once a week, with daily observations when a source was seen to be flaring.

3. Time-series analysis

The most variable features in a maser spectrum can be found visually by plotting the upper and lower envelopes of all of the spectra. This is calculated by finding the maximum and minimum value of the time-series in each spectrum. An example of such a plot is shown in Figure 1, which shows the range of variation in G351.78-0.54 for the period January 1999 to April 2003. One can select channels of interest from these spectra for further analysis.

Determining whether an astronomical time-series showing regular variations is periodic can be challenging. The samples are generally unevenly spaced, making it impossible to use a standard Fast Fourier Transform. A number of methods have been developed for period searches of unevenly sampled time-series. The most popular of these are phase dispersion minimisation or epoch-folding, the Discrete Fourier Transform (DFT) and the Lomb-Scargle periodogram. Additional challenges in the methanol data are long-term trends, non-periodic outbursts, flares of varying amplitudes and profiles that change with each repeat.

Epoch-folding using the test statistic developed by Davies (1990) is effective for short time-series, even when there are large gaps in the data. However, the data need to be detrended, which could potentially introduce a bias to the results. Various DFT algorithms were tried (Deeming, 1975; Scargle, 1982; Kurtz, 1985, Lenz & Breger 2005), but these had limited success since the variations were generally non-sinusoidal. The Lomb-Scargle periodogram (Press & Rybicki 1989) has proven to be the most effective in determining the underlying periods in the maser time-series. Long-term trends manifest as a very low-frequency sinusoid, which can be subtracted from the data before calculating a new periodogram. This also gives the potential to verify multiple periods in the data.

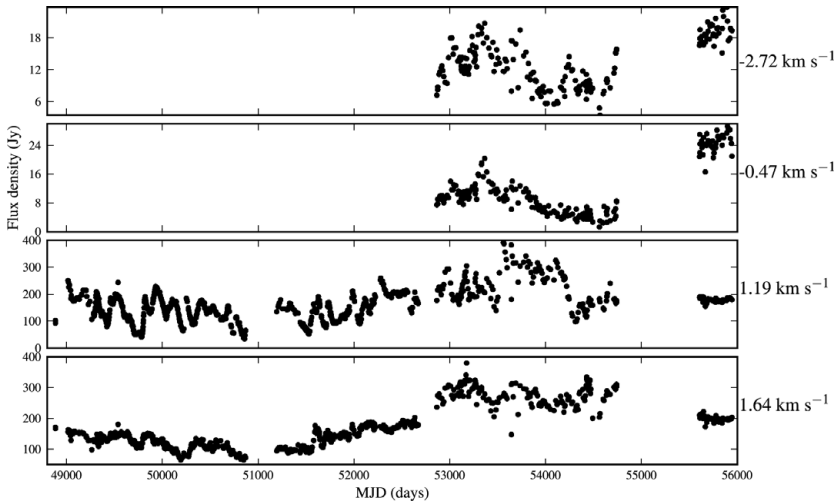


Figure 2. Time-series of G351.78-0.54 at 6.7 GHz.

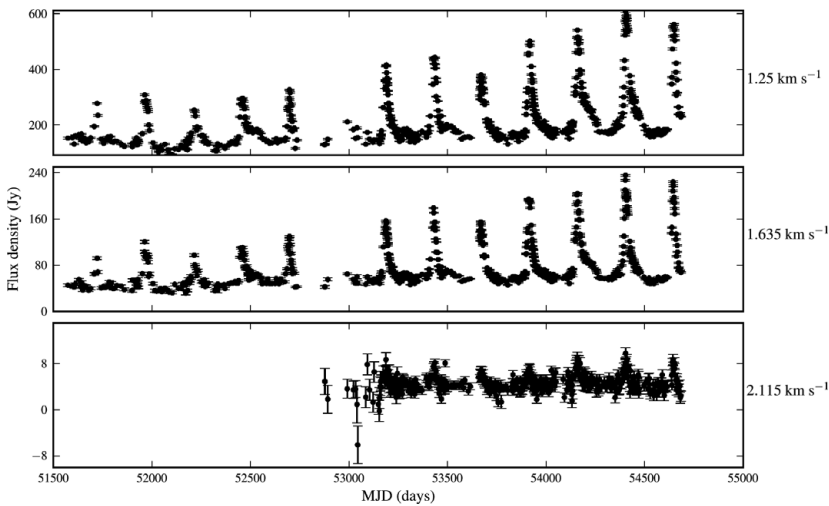


Figure 3. Time-series of G9.62+0.20 at 12.2 GHz.

4. Results

The range of variation and time-series of the dominant spectral features in G351.78-0.54 are shown in Figures 1 and 2. This source does not exhibit periodic behaviour but is highly variable. The most interesting characteristic is a time delay across the velocity features in the left-hand peak. It has been suggested by Macleod & Gaylard (1996) that this could be caused by an outflow passing behind the masers. LBA observations show that the masers do indeed show a strong position-velocity gradient (Goedhart *et al.* in prep).

The time-series of the most variable features in G9.62+0.20 at 12.2- and 6.7- GHz are shown in Figures 3 and 4, respectively. The flares have a period of 244 days. The

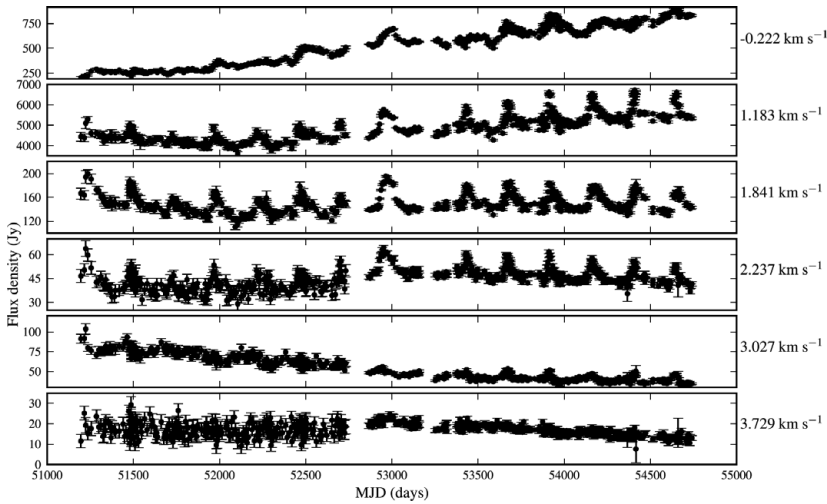


Figure 4. Time-series of G9.62+0.20 at 6.7 GHz.

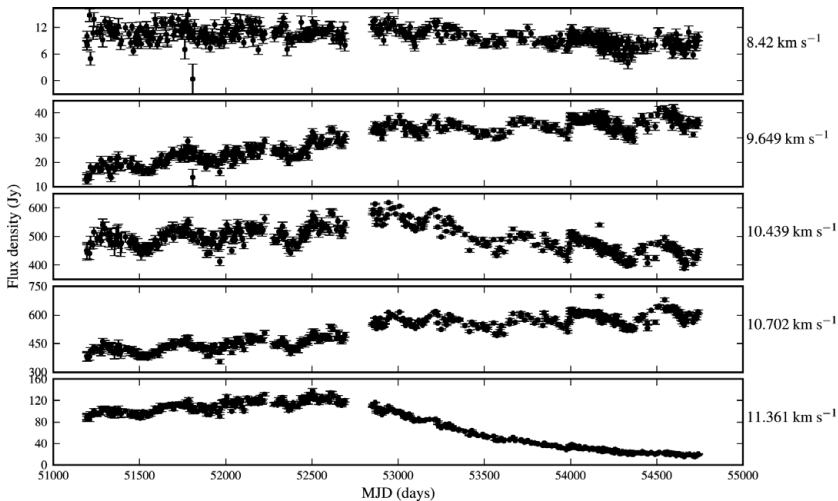


Figure 5. Time-series of G188.95-0.89 at 6.7 GHz.

12.2 GHz masers have been showing progressively stronger flares. Correlated flares are seen at 6.7 GHz, but they are not as strong. The baseline intensity between flares has remained relatively constant at 12.2 GHz, while some features at 6.7 GHz have shown steady increases (-0.22 km/s) or decay (3.027 km/s).

G188.95+0.89 (Figure 5) showed low-amplitude but clear sinusoidal variations in all its spectral features up to mid-2003. The period of 394 days can still be seen in the time-series but the cycle profile has changed to show a sharp rise and slow decay. The feature at 11.361 km/s has been showing a steady decay since 2003.

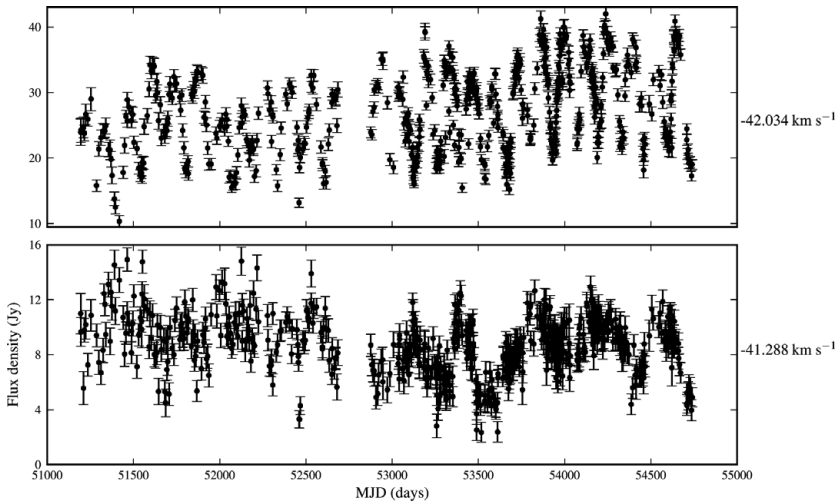


Figure 6. Time-series of G338.93-0.06 at 6.7 GHz.

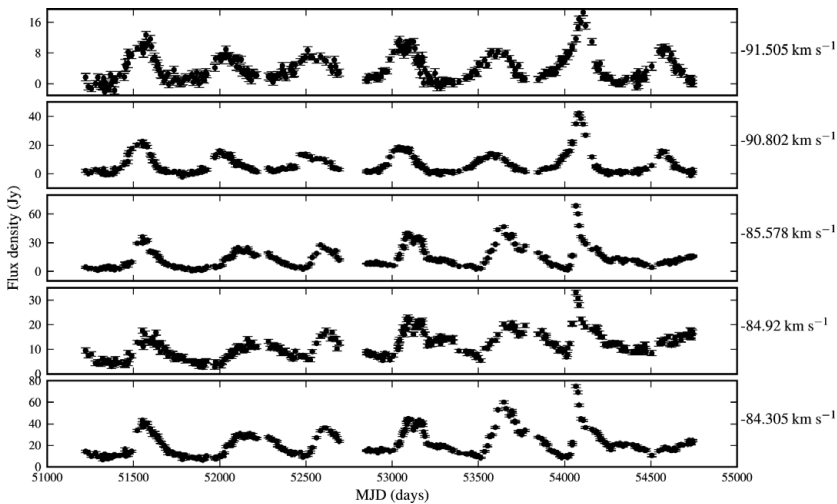


Figure 7. Time-series of G331.13-0.24 at 6.7 GHz.

G338.93-0.06 (Figure 6) shows a clearly defined period of 132.5 days in the feature at -42.034 km/s, but does not show correlated variability in the other feature at -41.288 km/s. The time-series is characterised by sharply defined minima.

The time series for the peak channels at 6.7 GHz in G331.13-0.24 is shown in Figure 7. All of the features show a periodic signature of 502 days. The group at -87 to -83.5 km/s show flares which start at regular intervals, but the duration of these flares varies, as well as the shape of the flares. Figure 8 shows the result of folding the time-series modulo 502.7 days. A time delay of ~ 70 days is apparent between the two velocity groups. The second group shows a well-defined minimum just before the start of the flares.

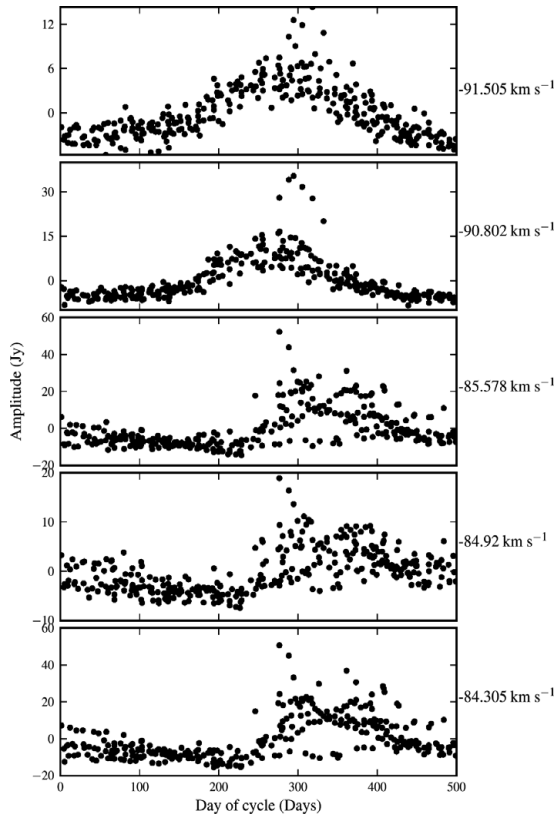


Figure 8. Time-series of G331.13-0.24 folded modulo 502.7 days.

G12.89+0.49 (Figure 9 has the shortest observed period of 29.4 days and shows a well-defined minimum just before the start of a flare, with flare amplitude and peak time varying from cycle to cycle.

G339.62-0.12 (Figure 10) and G328.24-0.55 (Figure 11) show very similar behaviour and similar periods of 202 and 222 days, respectively. Not all of the peaks show periodicity. The features at -37.178 and -35.729 km/s in G339.62-0.12 show additional, non-periodic flares, which presumably indicate localised changes in those particular maser features.

5. Discussion and conclusion

A wide range of periods and cycle profiles are seen. While the light curves do not appear to be strictly periodic, it is likely that there is an underlying periodic trigger, as indicated by the minima of the light curves which appear to be the most stable feature in the cycle profiles. Changes in cycle profile from flare to flare can be explained by varying conditions in the volume of masing gas (eg. changes in maser path length due to turbulence).

In van der Walt (2011) it was shown that the light curves for G9.62+0.20 and G188.95+0.89 can be explained by a simple colliding wind binary model, and the decay of the 11.361 km/s feature in G188.95+0.89 could be due to the recombination of the ionizing

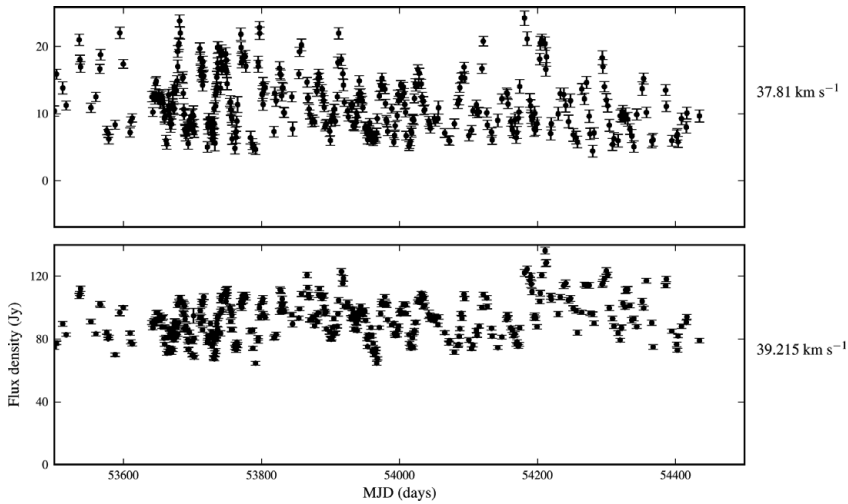


Figure 9. Time-series of G12.89 at 6.7 GHz. A subset of the full time-series is shown here for clarity.

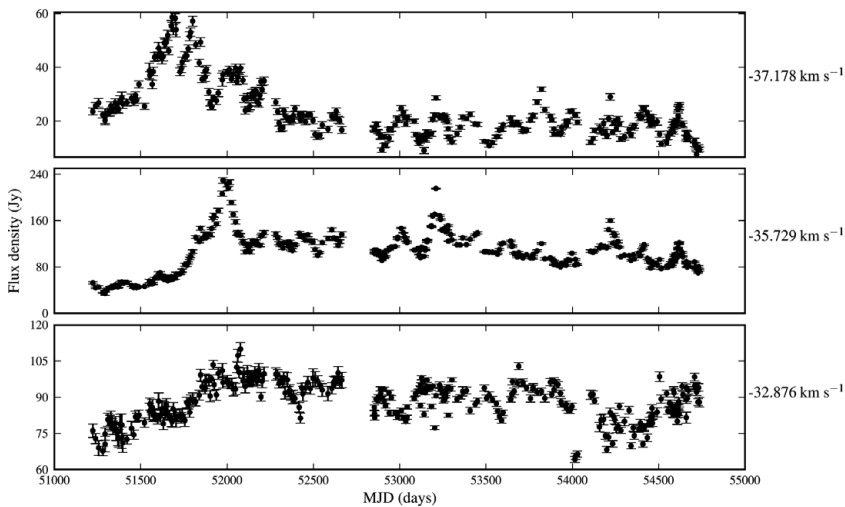


Figure 10. Time-series of G339.62-0.12 at 6.7 GHz.

gas in the background. Different light-curves can be reproduced by changing the orbital parameters of the binary system. Recently Szymczak *et al.*(2011) discovered a new periodic methanol maser source, G22.357+0.66 which has a period of 179 days and shows a similar flare profile to G9.62+0.20. Araya *et al.*(2010) detected another periodic source, G37.55+0.20, which exhibits correlated quasi-periodic flares in methanol and formaldehyde. In this case, the period of the flares appears to be getting shorter. They propose that the flares are caused by periodic accretion of circumbinary disk material.

Much more work needs to be done before the implications of periodic and quasi-periodic maser variability are understood. Observationally, further searches for periodic sources to increase the sample size will be helpful in characterising the properties of these sources.

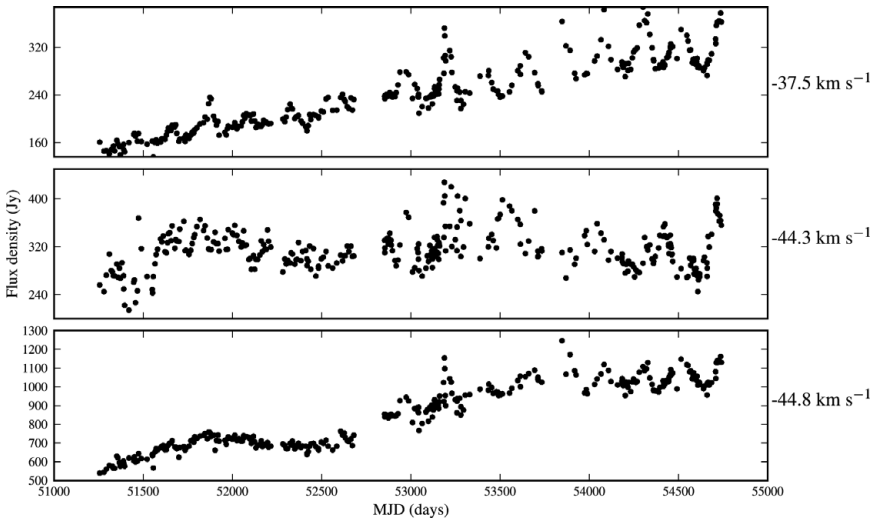


Figure 11. Time-series of G328.24-0.55 at 6.7 GHz.

High resolution, multi-wavelength maps are needed to understand the relation between the masers and other objects such as HII regions and outflows. Simultaneous monitoring of other maser lines will also be useful in understanding whether the root cause of the maser variability comes from the pump or background radiation. Detailed modelling will be necessary to understand the effects of radiative transfer in different morphologies and maser models with time-dependent components would have to be developed.

References

- Araya, E. D., Hofner, P., Goss, W. M., Kurtz, S., Richards, A. M. S., Linz, H., Olmi, L., & Sewio, M., 2010, *ApJ*, 717, L133
- Breen, S. L., Ellingsen, S. E., Caswell, J. L., & Lewis, B. E., 2010, *MNRAS*, 401, 2219
- Caswell, J. L., Vaile, R. A., & Ellingsen, S. P., 1995, *Proc. Astron. Soc. Aust.*, 12, 37
- Cragg, D. M., Sobolev, A. M., & Godfrey, P. D., 2005, *MNRAS*, 360, 533
- Davies, S. R., 1990, *MNRAS*, 244, 93
- Deeming, T. J., 1975, *Astroph. & Sp. Sc.*, 36, 137
- Goedhart, S., Gaylard, M. J., & van der Walt, D. J., 2004, *MNRAS*, 355, 553
- Kurtz, D. W., 1985, *MNRAS*, 213, 773
- Lenz, P. & Breger, M., 2005, *Communications in Asteroseismology*, 146, 53
- MacLeod, G. C. & Gaylard, M. J., 1996, *MNRAS*, 280, 868
- Press, W. H. & Rybicki, G. B., 1989, *ApJ*, 338, 277
- Scargle, J. D., 1982, *ApJ*, 263, 835
- Szymczak, M., Wolak, P., Bartkiewicz, A., & van Langevelde, H. J., 2011, *A&A*, 531, L3
- van der Walt, D. J., 2011, *AJ*, 141, 152